



Synthesis and characterization of eugenol-based poly (benzoxazine –PU) with glycine ethylester core copolymer coating for corrosion protection on mild steel

JAYANTHI KANNAIYAN^{1*} and SIVARAJU MANI²

^{1*} Assistant Professor, Post Graduate & Research Department of Chemistry, Queen Mary's College(A), Chennai – Pincode 600004, Tamil Nadu, India.

² Assistant professor, Post Graduate & Research Department of Chemistry, Thiruvalluvar Government Arts College, Rasipuram, Pincode 637401, Tamil Nadu, India.

* Corresponding author: kjayanthi_che@queenmaryscollege.edu.in

ABSTRACT:

In this study, we will be discussing the effect of isocyanate on the anti-corrosive property of the mild steel by the co-polymerization of urethane with benzoxazine, which was synthesized from eugenol, glycine ethyl ester and paraformaldehyde. Monomer was characterized by proton, carbon NMR, Fourier Transform-IR and Ultraviolet- visible techniques. Similarly, the co-polymer was also characterized by Fourier Transform-IR and Ultraviolet- visible techniques. The polymerization process was conducted on the mild steel surface by dip-coating of the benzoxazine with isocyanate hardener in three ratios i.e., 60%, 80%, 100% and cured in a muffle furnace. Then, the coated mild steel was investigated for the anti-corrosive property using Polarization and Electrochemical Impedance Spectroscopy. The results show that the rise in the amount of isocyanate hardener on the metal surface will elevate the corrosion inhibition efficiency. The morphological studies and elemental analysis performed by using SEM- EDAX. The hydrophobicity of the copolymer was investigated by usual ASTM-D570 methods like water absorption and Gel absorption studies. The theoretical studies DFT was also performed to support the anti-corrosive property of the synthesized monomer and its copolymer in terms of the band gap, electrophilicity factors.

KEY WORDS:

Anti-corrosive coating, Eugenol, glycine ethyl ester, polybenzoxazine, Isocyanate, Band gap and Electrophilicity.

INTRODUCTION:

Corrosion is electrochemical destructive phenomena which is a major problem, causing considerable amount of loss of material. It is estimated that corrosion costs the global economy more than US\$2.5 trillion annually [1]. Most of the heterocyclic compounds can

acts a corrosion inhibitor for the steel and other metals [2] because of its adsorption on the metal surface due to the presence of rich pi electron density around the heteroatom like N, P, O and S [3-5]. Environment friendly plant extract can also act as an efficient corrosion inhibitors [6, 7] due to the presence of electron rich heteroatoms. Nanotechnology has been more crucial during the past 20 years in advancing creative technical solutions to control corrosion [8], Admiration of agro-food wastes has garnered attention as a source of "green" chemicals for the development of sustainable chemistry that may minimise the effect profits for the environment, produce profits for the of anti-corrosion protection sector, and minimises their negative environmental consequences [9]. The conducting polymers like, polypyrrole [10], polyfuran [11], polyaniline [12], polythiazoles [13], etc., can be easily synthesized and widely accepted an efficient inhibitor on the metal surface.

Excellent polymer coating materials must have high hydrophobicity, low water absorption, high cross-link density and ionic resistance, and good adhesion in order to effectively inhibit the permeation of electrolytes into the coating/metal interface and prevent a corrosion reaction. Polybenzoxazine exhibit these properties, so that many research work on the corrosion inhibition were conducted with these polymers[14, 15]. Few interesting facts about this polymer is, it does not need an initiator or catalyst, thermally accelerated ring-opening, nearly low shrinkage, tractability, and the absence of harmful by-products are the key characteristics of the polymerization of benzoxazine monomers. Previously polybenzoxazine synthesized from bisphenol-A as the starting material, it showed some disadvantages as a coating material, to replace the BPA, many other eco-friendly phenols were used for the synthesis of polybenzoxazine.

Yuzhu Cao et.al., fabricated a bio-based polybenzoxazine super hydrophobic coating on the carbon steel using cardanol as the phenol [16]. Ruhi Yang et.al., synthesised a bio-based high-performance tri-furan functional benzoxazine from guaicol and reported the above polymer possessing high thermal stability with good flame-retardant properties [17]. Ganesh. A. Phalak et.al., synthesised benzoxazine from guaiacol and copolymerise it with polyurethane and reported anti-corrosive property of the above with 99% corrosion efficiency [18]. Madalina et.al., synthesised benzoxazine from eugenol and vanillin and grafted this with polyethyleneimine backbones and reported its fire- retardant properties [19]. Sini et.al., prepared bis-benzoxazines from vanillin feed stock with good thermal adhesion properties [20].

Interestingly, polyurethanes were created by combining polyols and isocyanates with the right catalyst to boost the hydrophobicity and chemical resistance of the metal surface. As

a result, numerous advances were made in the use of polyurethane in anti-corrosive coatings. Zhu et.al., developed a super hydrophobic coating on a metal surface through one-step spray coating using benzoxazine, polyurethane and mesoporous SiO₂ and report by increases the polyurethane content in the coating will enhances the hydrophobicity thereby it restricts the water particle to enter the metal surface thereby it controls the corrosion on it [21]. Sreelakshmi et.al., also synthesised a no catalyst, solvent free colourless cardanol based PU coating which is copolymerised with hydroxy- terminated polydimethylsiloxane [22]. In order to synthesise a new hydrophobic benzoxazine- polyurethane coating on mild steel, in this research we have synthesise a new benzoxazine precursor from eugenol, paraformaldehyde and glycine ethyl ester which is copolymerised with hexamethylene diisocyanate in different ratios and discussed its anti-corrosive studies in 3.5% NaCl medium because of the world consists of 70% water which contains the natural electrolyte of sodium chloride of the above mentioned percentage.

2. Materials and Methods:

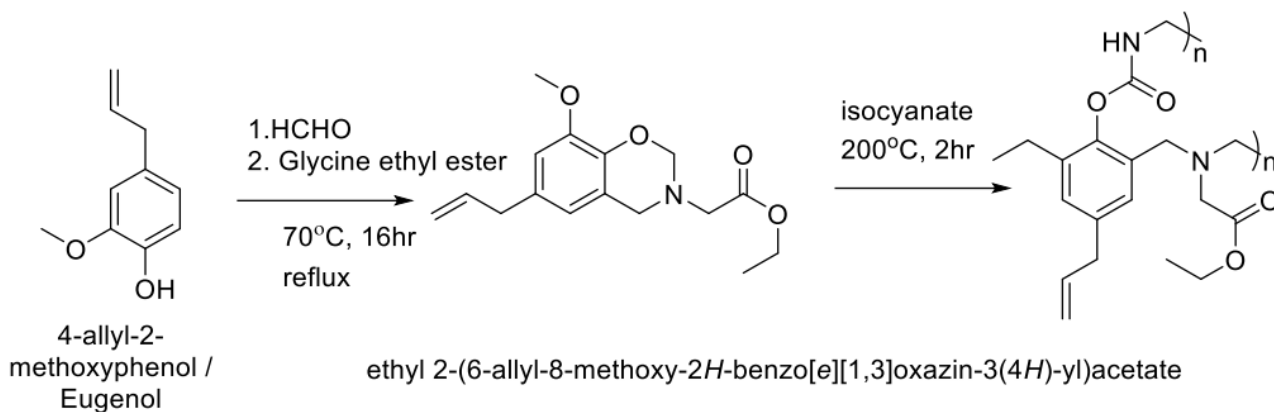
2.1. Synthesis of ethyl 2-(6-allyl-8-methoxy-2H-benzo[e][1,3]oxazin-394H)-yl)acetate:

Glycine ethyl ester (0.85g, 6.09mmol), paraformaldehyde (0.383g, 12.789mmol), and 10mL of CHCl₃ were added to a 250ml three-neck RB flask. The mixture was then agitated at 50°C for 30 minutes. Eugenol (0.943 mL, 6.090 mmol) diluted in 25 mL of CHCl₃ was added to the solution after 30 minutes, and it was agitated for 16 hours at 70°C. 100 mL of chloroform was added to the reaction mixture before filtering, and TLC was used to monitor the reaction's development. Following the conclusion of the response, to eliminate unreacted phenols and water on the organic layer, the filtrate was then washed with water, brine solution, and 1N sodium hydroxide. After that, it was taken out from organic layer and dried over anhydrous sodium sulphate. When the solvent evaporated, the monomer's yellowish-brown liquid was Obtained.

2.2. Copolymerisation of benzoxazine with isocyanate hardener:

The above synthesized monomer was dissolved in 1,4-dioxane, to that solution isocyanate hardener in toluene was added. Three combinations of isocyanate with benzoxazine were prepared, the three combinations are in the ratio of benzoxazine (EuBz-gly): polyurethane (PU) 100:60, 100:80, 100:100. The emery paper was used polish the metal

surface to improve the adhesion on mild steel plates and then the plates were cleaned by using water, hexane and acetone to remove impurities. The cleaned MS was then coated with BZ: PU solution using the dip-coating technique for 1 min, and then was slowly removed from it at a speed of 100 mm/min.. The coated MS was then thermally dried and cured in a furnace for three hours at 200°C. The coated mild steel was the main topic of the EIS investigation.



Scheme- 1: Synthesis and polymerisation of ethyl 2-(6-allyl-8-methoxy-2H-benzo[e][1,3]oxazin-3(4H)-yl)acetate and its copolymerisation with polyurethane

2.3. Characterization techniques:

A "Thermo Scientific Nicolet iS50 FT-IR Spectrometer" was used to analyse the IR spectrum, while a "Labman LMSP UV-1200 UV-Vis" was used to analyse the UV spectrum. Dimethyl sulfoxide-D₆ was used as the solvent in a "Bruker 500 MHz" ¹H NMR" observation of the monomer. Additionally, a "Bruker 125 MHz" equipment was used to record ¹³C NMR" for the same sample. To verify the product generation, thin layer chromatography (TLC) was used. Using the "JEOL JSM 6390" scanning electron microscope and a 20 keV energy acceleration beam, the surface is examined.

2.4. Corrosion Studies- Tafel Polarization experiment and Electrochemical Impedance Spectroscopy (EIS) experiments:

The polarisation studies were conducted using the Biologic SP 300 model machine, which has three electrodes with Ag/AgCl serving as the reference electrode and Pt serving as the counter electrode. The corrosion rate, corrosion efficiency and free energy of adsorption (ΔG_{ads}) was calculated using the I_{corr} value from Tafel extrapolation from equation (1, 2 & 3) and the R_{ct} value obtained from the Nyquist plot from the equation (4) [18 & 23].

$$CR = \frac{I_{corr} \times K \times EW}{\rho A} \text{ mmpy} \quad (1)$$

Where, CR= Corrosion Rate, EW= 27.9g, K= 3272 mmpy (CR constant), ρ = 7.85 g cm⁻³ (material density) and A= 1cm² (Area of the sample).

$$CE (\%) = \left[\frac{I_{corr}(b) - I_{corr}(c)}{I_{corr}(b)} \right] \times 100 \quad (2)$$

Where, CE= Corrosion Efficiency or Inhibition efficiency, I_{corr} (b)= Corrosion current for the uncoated Mild steel, I_{corr}(c)= Corrosion current for the coated mild steel.

$$(\Delta G_{ads}) = -RT \ln(55.5 K) \quad (3)$$

Where, K= equilibrium constant, which is calculated from, $\left(\frac{\theta}{c(1-\theta)}\right)$, θ = Surface coverage, C = Concentration of inhibitor in mole/ lit and 55.5 represents the concentration of water in mol/lit.

$$CE (\%) = \left[\frac{R_{ct}(c) - R_{ct}(b)}{R_{ct}(c)} \right] \times 100 \quad (4)$$

Where, R_{ct} (c) = coated mild steel's charge transfer resistance, R_{ct} (b)= uncoated mild steel's charge transfer resistance.

2.5 Computational studies - Density Functional Theory (DFT)

Density functional theory was used to examine the computational computations and representation of HOMO and LUMO using the Gaussian 09W programme. The chemical structure of the monomer was optimised on the basis of the B3LYP/6.31 G basis set. The calculated structures of the HOMO, LUMO, and MEP (molecular electrostatic potential) representations were seen using the Gauss view software programme.

2.6. Studies on Water absorption.

By using the ASTM D570 procedure, samples that had been coated and cured with monomer and copolymers were submerged in water for 24 hours to determine their hydrophobicity [18]. Prior to the immersion, the weight of the cured samples was recorded (W_b). The water particles are drained with a paper towel and taken out after 24 hours. The samples' weight (W_a) was then recorded. Weight difference was used to determine the water particles' percentage of absorption from the equation (5).

$$WA (\%) = \left[\frac{W_a - W_b}{W_b} \right] \times 100 \quad (5)$$

Where, WA= Water absorption, Wa= Weight of the coated and cured mild steel after the immersion of water, Wb= Weight of the coated and cured mild steel before the immersion of water.

2.7 Studies on Gel absorption

The gel absorption of monomer and every coated, cured copolymer sample was calculated during the whole research using the weighing method. Prior to the inquiry, each sample's weight (Wb) was recorded [18]. The samples were taken out of the xylene after 24 hours of immersion at room temperature and dried in an oven under vacuum. Following this procedure, the weight of each sample was once more recorded for (Wa). The proportion of gel formation in the copolymer was estimated from the weight differential between the two above, namely Wa and Wb from the following equation (6).

$$GA (\%) = \left[\frac{W_a}{W_b} \right] \times 100 \quad (6)$$

Where, GA= gel absorption, Wa= Weight of the mild steels after the immersion of xylene, Wb = Weight of the mild steels before the immersion of xylene.

3. RESULTS AND DISCUSSION

3.1 NMR spectrum of ethyl 2-(6-allyl-8-methoxy-2H-benzo[e][1,3]oxazin-394H)-yl) acetate:

To confirm the structure of the monomer ethyl 2-(6-allyl-8-methoxy-2H-benzo[e][1,3]oxazin-394H)-yl)acetate “¹H NMR and ¹³C NMR” analysis was employed. From the figure-1, the three alkyl protons (-COO-CH₂-CH₃) from the glycine ethyl ester were appeared in the aliphatic region from 1.248ppm to 1.3ppm, similarly the two protons from the -COO-CH₂-CH₃ unit, were appeared 4.192ppm to 4.228ppm. The two protons from -N-CH₂-COO- unit peak appeared at 3.281 ppm to 3.328 ppm. Five protons from allyl group attached to the eugenol ring appeared at the region 3.281, 5.113 and 6.0 ppm. Two aromatic protons in the aromatic ring appeared in the region 6.4 and 6.5ppm [24, 25]. Methoxy protons on the aromatic ring observed at the region 3.876 ppm. The peaks appeared in the region 4.078 ppm and 4.965 ppm are respective for four protons from the benzoxazine ring which confirms the benzoxazine formation. Following the integration, 21 protons were accounted. Furthermore, ¹³C-NMR provides accurate details of monomer's structure. The alkyl methyl carbon (-COO-CH₂-CH₃) from the glycine ethyl ester were appeared in the aliphatic region 14.3 ppm, the -CH₂-carbon (-COO-CH₂-CH₃) were appeared at 110.1ppm due to it is attached to the

electronegative oxygen atom. Similarly, the allyl carbons on the eugenol ring (-CH₂-CH=CH₂) shows their chemical shift at 40.06, 137.5 and 115.6 ppm respectively. The peaks at the region 137.9, 130.8, 147.3, 147.7, 122.2 and 119 ppm were responsible for the aromatic carbon moieties [26, 27]. The methoxy carbon on the aromatic ring shows its chemical shift in 55.9 ppm and the benzoxazine ring carbons chemical shift at the region 50.7 (Ar-CH₂-N-) and 82.2 ppm (-N-CH₂-O-) which also conforms the benzoxazine formation. The carbonyl carbon from the glycine ethyl ester carbon appeared at the region 170.8ppm which was shown in the figure 2. Hence, from NMR analysis the monomer structure shown in the scheme-1 was confirmed.

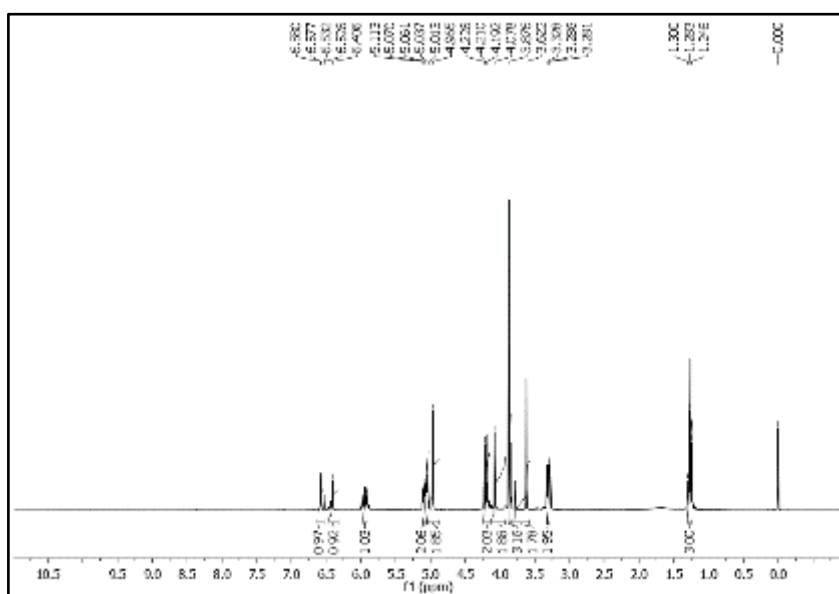


Figure 1: ¹H NMR spectrum of ethyl 2-(6-allyl-8-methoxy-2H-benzo[e][1,3]oxazin-3(4H)-yl)acetate

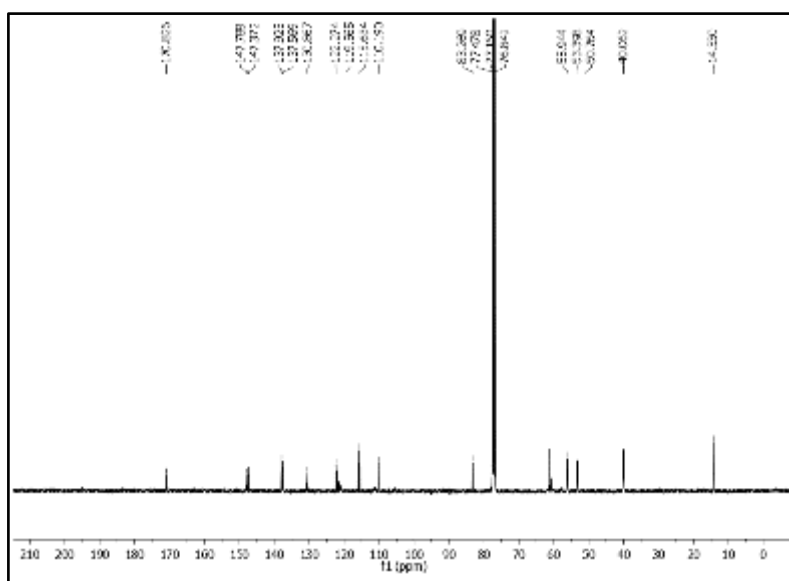


Figure 2: ^{13}C NMR spectrum of ethyl 2-(6-allyl-8-methoxy-2H-benzo[e][1,3]oxazin-3(4H)-yl)acetate

3.2 IR spectrum of pure EuBz-gly and blends with EuBz-gly-PU

Figure 3 depicts the "FT-IR spectra" of the monomer and all copolymers formed from the monomer and an isocyanate hardener. The symmetric and the asymmetric stretching of the -CH from the $-\text{CH}_2$ of the formed benzoxazine and the eugenol side chain appeared at 2945 and 2857cm^{-1} . The existence of 1° and 2° amine groups was ruled out at higher wavenumbers since no stretching frequencies were seen, but the presence of 3° amine is verified because the heteroatom was free of any other labile protons. The asymmetric stretching frequency of -C-O- is represented at 1205cm^{-1} band, while the symmetric stretching is represented by the band at 1215cm^{-1} . The band at 920cm^{-1} confirms the formation of a benzoxazine ring [26-29]. Other aromatic -CH band appeared at 1454cm^{-1} and the band at 3357cm^{-1} represents the -N-H stretching frequency, which is present in the polyurethane attached to the polybenzoxazine. A peak at 1676cm^{-1} corresponds to the carbonyl group from the benzoxazine monomer and this peak was strongly visible as a result of polyurethane incorporation into our monomer.

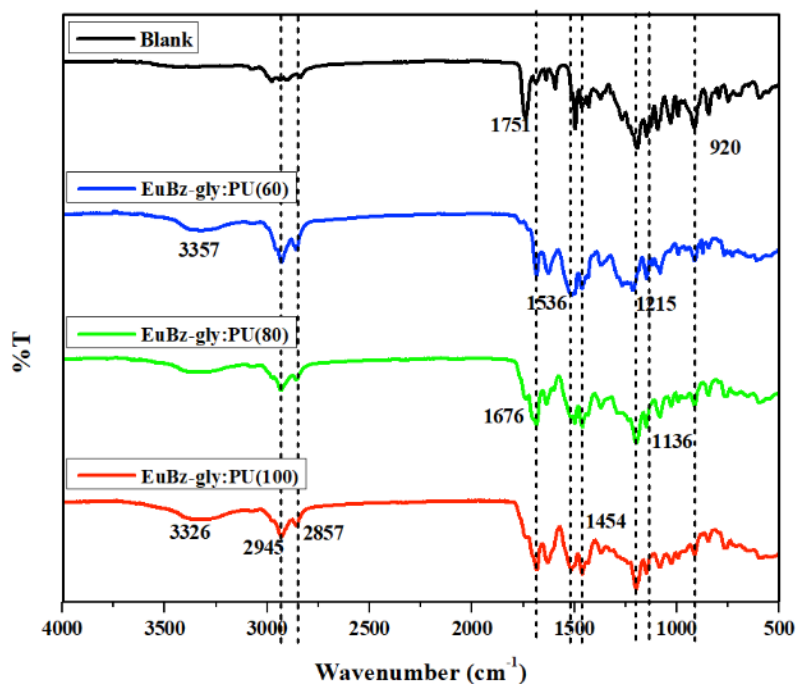


Figure3: FTIR spectrum of benzoxazine synthesised from eugenol and glycine ethyl ester and its copolymers with polyurethane in three ratios

3.3 VaBz monomer and VaBz-gly-PU blends' UV-Vis spectrum:

From the figure- 4, we observed that the faint bands at 250 nm and 284 nm that the monomer displays are due to the electronic transition $p - p^*$. The eugenol-based benzoxazine with

isocyanate loading exhibits two peaks at 269 and 283 nm that are attributable to the p - p* and n - p* transitions [30, 31]. Observed an alteration in the p - p* band during the copolymerization with isocyanate. The band that corresponds to the n - p* transition also increased its absorbance, clearly demonstrating how significantly the isocyanate induced the monomer's electronic transition.

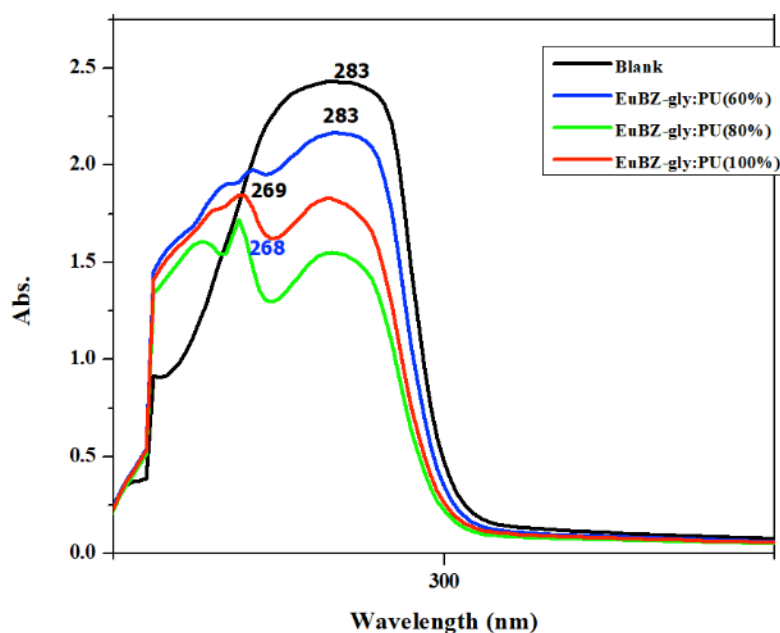


Figure:4 UV spectrum of benzoxazine synthesised from eugenol and glycine ethyl ester and its copolymers with polyurethane in three ratios

3.4 Corrosion Studies

3.4 a. Electrochemical studies by “Potentiostatic Polarization”:

Figure 5 depicts the Tafel polarisation curves for the coated and dried copolymers of benzoxazine made from eugenol and urethane. "Superimposing the straight line along a linear portion of the anodic or cathodic curve" was used to determine the I_{corr} and E_{corr} values. Typically, a destructive metal with a high corrosion current (I_{corr}) allows for frequent electron mobility, which makes the metal corrode readily and results in a high rate of corrosion on the metal's surface. On the other hand, more, positive value of corrosion potential (E_{corr}) represents less corrosion rate [32-34]. Based on this knowledge, the Tafel data for the eugenol-based benzoxazine and related copolymers were listed in Table 1 with various concentrations. In either case, the uncoated mild steel exhibits a higher I_{corr} value and a lower E_{corr} value, indicating that more corrosion has occurred on it. The corrosion

potential and current of mild steel that has been coated and dried with eugenol-based benzoxazine copolymerized with urethane are improved. The EuBz-gly: 60% PU coated material attained I_{corr} and E_{corr} value of 0.0063mA and -624mV respectively, this was enhanced to 0.0000013mA and -538mV by increasing the isocyanate to 80% (EuBz-gly: 80%PU), further which was enhanced to 0.0000001mA and -506mV by coating with EuBz-gly: 100%PU. From this we clearly demonstrate that the rate of corrosion on mild steel decreased as the amount of urethane increased. This is because more urethane causes the benzoxazine to produce an efficient noble layer for the metal surface by increasing its crosslinking capacity. 60% urethane coated shows 98.87% corrosion efficiency than the uncoated mild steel, 80% and 100% urethane coated shows 100% corrosion efficiency. The polymeric material's physisorption onto the metal surface prevented corrosion, according to the free energy of adsorption (DG_{ads}).

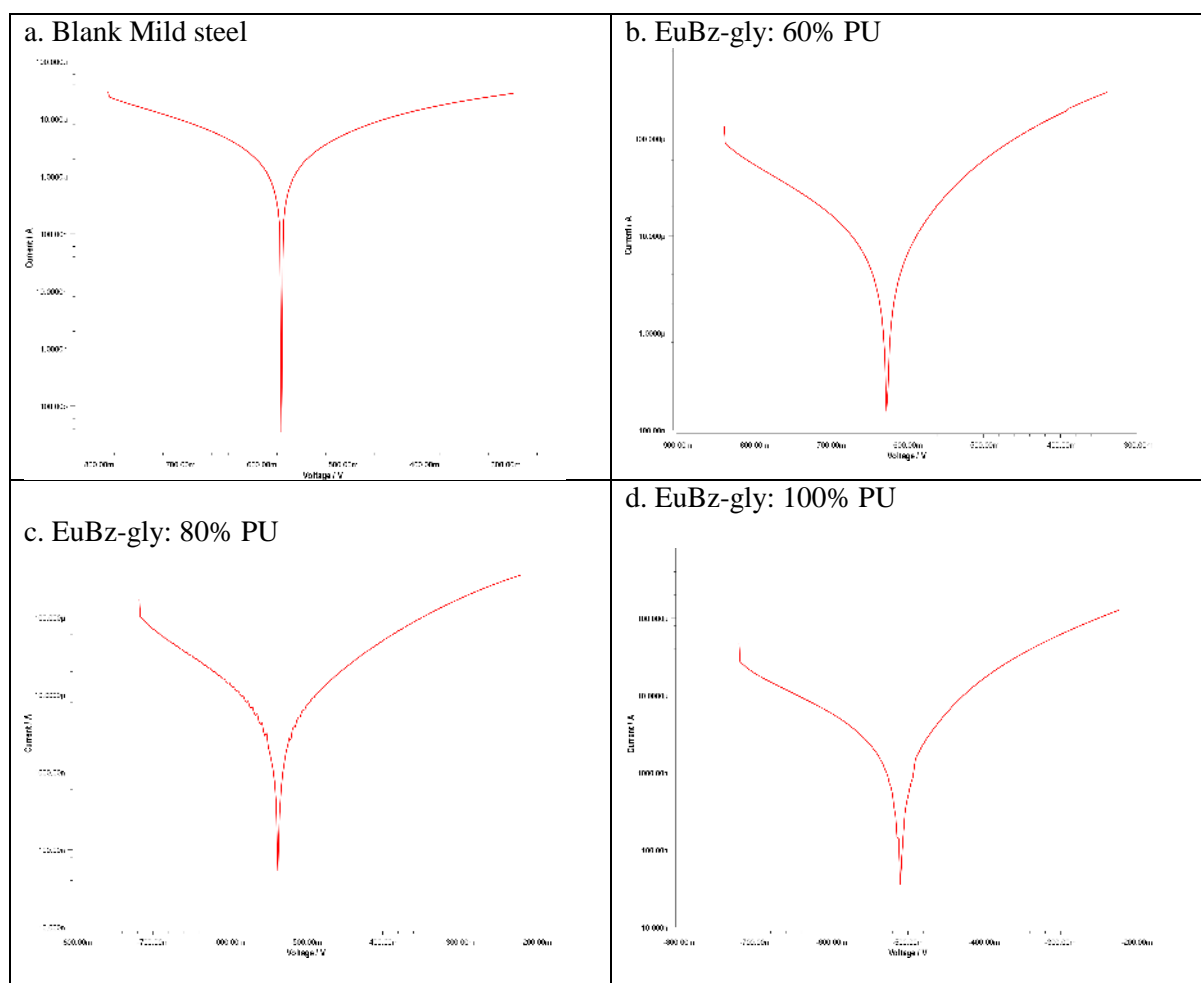


Figure 5: Tafel Plot for (a) Blank Mild steel, (b) EuBz-gly: 60% PU, (c) EuBz-gly: 80% PU and (d) EuBz-gly: 100% PU coated Mild steel respectively

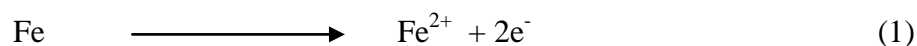
Table 1: Parameter calculated from the Tafel experiment

	I _{corr} (μA)	E _{corr} (mV)	Corrosion Rate (empty)	Surface Coverage (θ)	Corrosion Efficiency (%)	Tafel Constant		ΔG (ads) KJ/mol
						β _a mV/dec	-β _c mV/dec	
Blank	0.475	-574	5524			61.1	-60.5	
100:60(EuBZ-gly:PU)	0.0063	-624	73	0.9867	98.67	-136	132	-21.93
100:80 (EuBZ-gly: PU)	0.0000013	-538	0	1.0000	100.00	-207	171	-42.30
100:100(EuBZ-gly: PU)	0.0000001	-506	0	1.0000	100.00	-172	131	-48.12

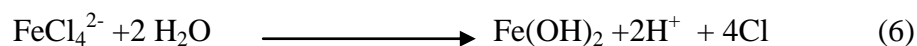
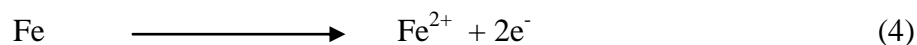
3.4b Electrochemical system behaviour of BZPU coatings:

The EIS method is one of the greatest methods for figuring out a material's resistivity. The results for the blank and the EuBz-gly:60%PU, EuBz-gly:80%PU, and EuBz-gly:100%PU coated and cured mild steel were given in the table-2. The EIS for our samples was recorded in 3.5% sodium chloride solution. The Nyquist plot, shown in Figure 6, includes two-timed constants that are represented by an inductive loop at low frequencies and a depressed capacitive semicircle at higher frequencies. While later corrosion constant is connected to the finding of an intermediate corrosion product, earlier corrosion constant is related to charge transfer. The two-time constants on the Nyquist plot are an inductive loop at lower frequencies (semi-circle) and a depressed capacitive semicircle at higher frequencies, respectively. These two-time constants are primarily caused by the adsorption of a corrosion reaction with an inhibitor reaction intermediate. R_s is a resistor associated with solution resistance, and charge transfer resistance is a measure of electron transfer over the surface that is directly derived from the semi-circle's diameter from the Nyquist plot and is inversely proportional to the rate of corrosion. Corrosion efficiency was calculated using the R_{ct} values of coated and uncoated mild steel. The R_{ct} value rises when more urethane is applied to mild steel, based on the data from the Nyquist plot. The capacitance of the double layer, another component, provides an explanation for the materials' electrochemical characteristics. (C_{dl}) [35-37] In addition, the constant phase element (CPE) rather than the ideal electrical capacitance is utilised in the model to mimic the impedance behaviour of the electrical double layer. According to Table 2, when compared to metal (mild steel) coated with EuBz-gly:PU, uncoated mild steel has a higher value of C_{dl}. It is evident that using 80% and 100% loaded urethane in the coating lowers the C_{dl} value even further because it increases the thickness of the electrical double layer or increases the local dielectric constant close to the metal surface.

The corrosion of the uncoated mild steel is due to the lack of the formation of insoluble thin oxide passive layer on its surface. The oxide layer isolated the mild steel from the aggressive environment. The formation of passive oxide layer is given by,



The chlorides attack the metal through the oxide layer and accelerates the corrosion of the metal. The effect of chloride ions on the mild steel is shown by the following reactions, (52)



The self-generating chloride ions propagates the corrosion process on the mild steel surface. The chloride concentration on the metal surface is decreased by coating of our eugenol based benzoxazine loaded with polyurethane. This is achieved by the forming an protective layer around the metal because of the presence electron donating heteroatoms such as N and O from the EuBz-gly:PU moieties. In presence of this coating the chloride ions fail to penetrate the mild steel surface thereby the inhibition efficiency increased, which was proved by the increased R_{ct} and decreased C_{dl} values of the coated mild steel compared with uncoated mild steel.

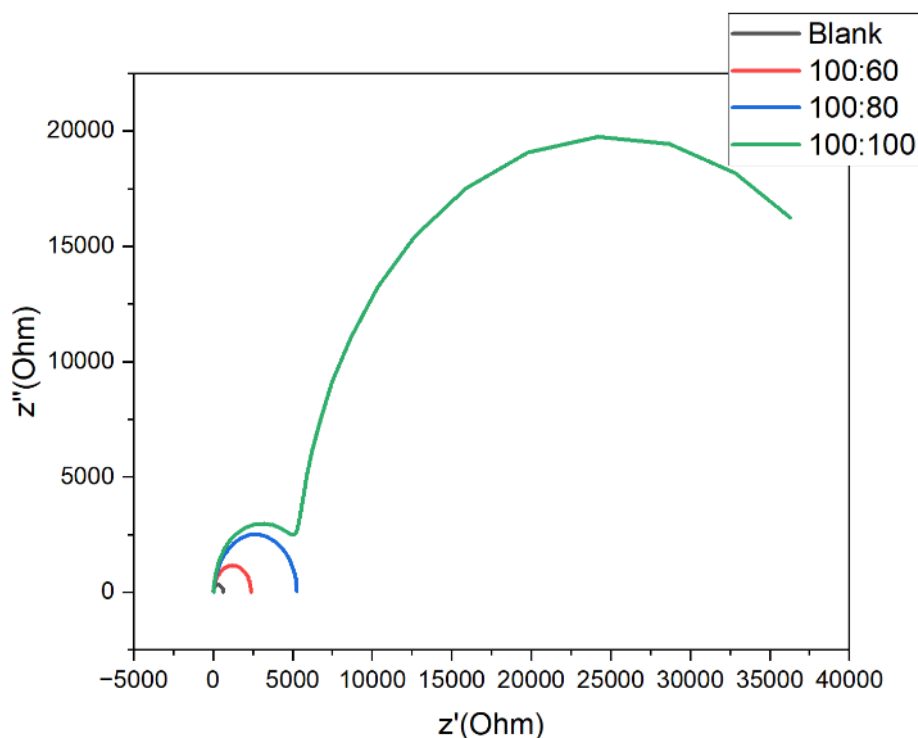


Figure6: NyquistPlot for (a) Blank Mild steel, (b) EuBz-gly: 60% PU, (c) EuBz-gly: 80% PU and (d) EuBz-gly: 100% PU coated Mild steel respectively

Table 2: Parameter calculated from the Nyquist plot

Concentration of coatings	Rect Ωcm^2	Cdl F/cm^2	Inhibition Efficiency (%)
Blank	647	7.150×10^{-9}	
100:60 (EuBZ-gly:PU)	2330	34.2×10^{-9}	72.23
100:80 (EuBZ-gly: PU)	5272	23.54×10^{-6}	87.73
100:100 (EuBZ-gly: PU)	44813	12.39×10^{-6} and 211.41×10^{-6}	94.80

3.5 Scanning microscopic analysis

SEM and energy-dispersive X-ray analysis (EDAX) were used to examine the surface morphology of mild steel before and after a week of immersion in 3.5% NaCl. Findings in Figure 6 demonstrate that mild steel without a coating has a flat surface that is susceptible to corrosion when immersed in a salt chloride solution. This gives the surface area a rough appearance [38,39]. The coating of the newly developed, eugenol-based benzoxazine, which was copolymerized with urethane, decreased the corrosion of mild steel. In particular, the

corrosion was greatly decreased by increasing the quantity of polyurethane from EuBz-gly100: PU60 to EuBz-gly100: PU100. After corrosion, mild steel coated with EuBz-gly100: PU60 displays a polished surface in contrast to blank mild steel, and this may be improved by the sample with EuBz-gly100: PU80. The mild steel's EuBz-gly100: PU100 coating, which has an even more polished surface than EuBz-gly100: PU80, also contributed to its improvement. This might be used as additional proof that mild steel with higher polyurethane content has improved corrosion resistance. This was further demonstrated by the EDAX analysis, as seen in figure 7. It is obvious from it that adding polyurethane to the surface decreased the amount of iron degradation after being exposed to 3.5% NaCl.

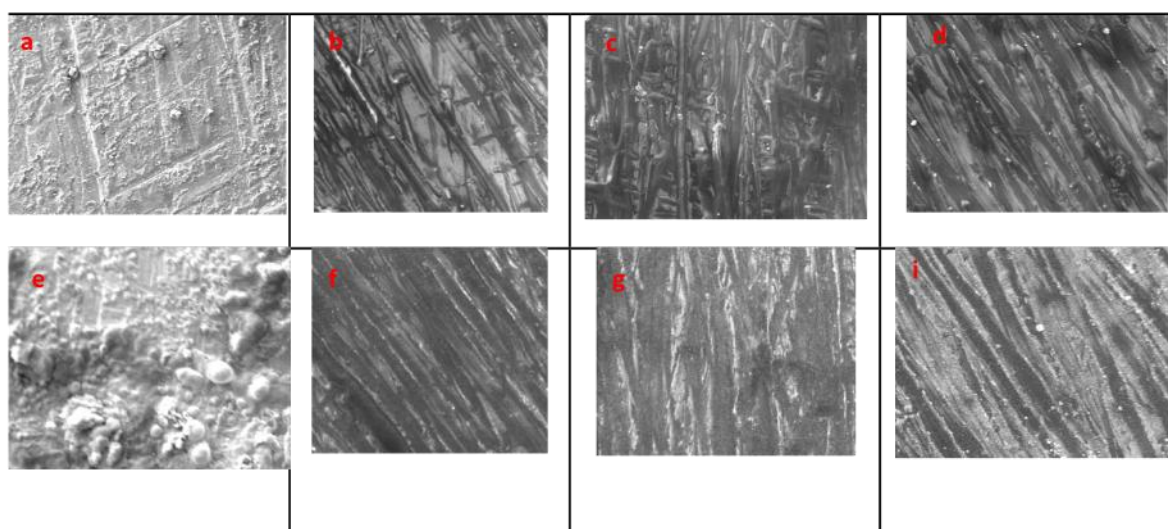
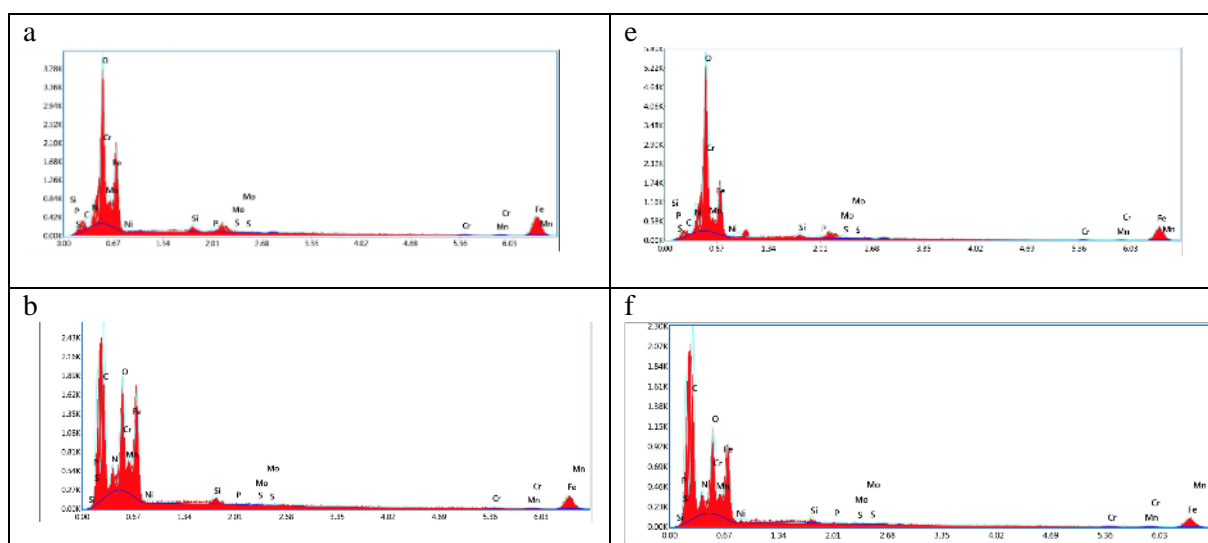


Figure 6: SEM Images of the before (a-d) and after (e-f) corrosion of samples blank (a and e), EuBz-gly:60%PU (b and f), EuBz:80%PU (c and g) and EuBz:100%PU (d and h)



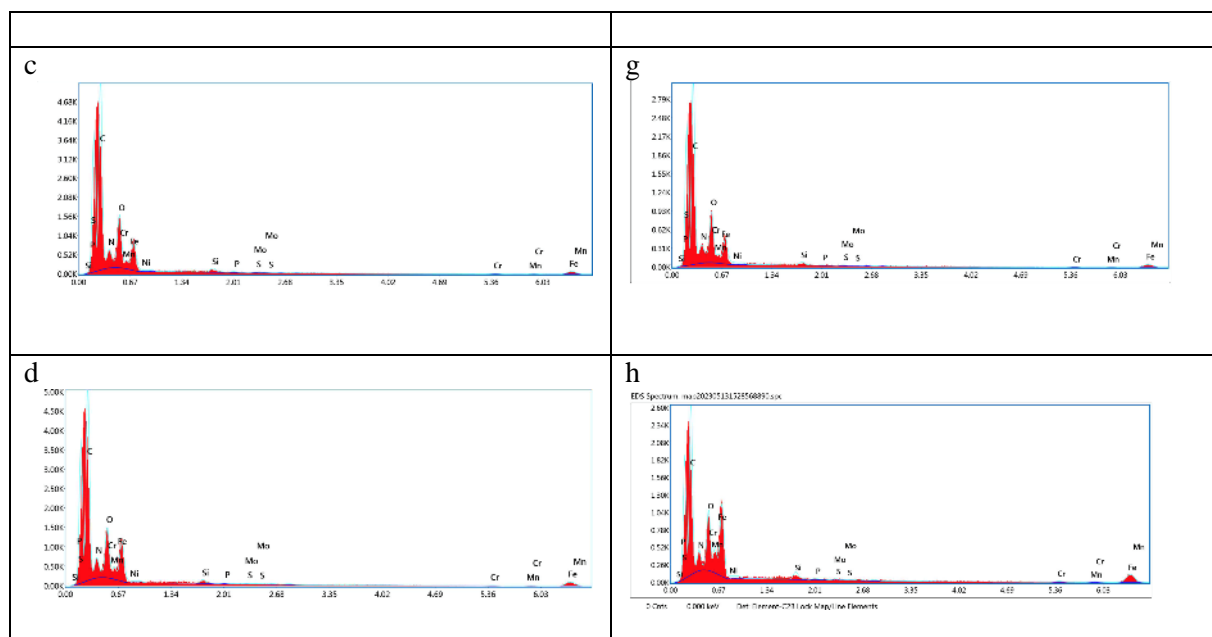


Figure 7: EDAX images of the before (a-d) and after (e-h) corrosion samples of blank (a and e), EuBz-gly:60%PU (b and f), EuBz-gly:80%PU (c and g) and EuBz-gly:100%PU (d and h)

3.6 Water adsorption studies:

The hydrophobic nature of polymer materials, which was impacted by the material's branching and cross-linking capabilities, is crucial to their anticorrosive properties. This hydrophobic feature was also affected by the addition of coating chemicals like urethane, which produced the cross-linking property through hydrogen bonding. It is clear from the figure-8 that as polyurethane concentration increases, the coating's ability to absorb water decreases significantly. The amount of water absorption in the eugenol-based benzoxazine was approximately 2.09%; this was reduced on mild steel by adding 60% polyurethane, again by adding 80% polyurethane, and further reduced by adding equal amounts of benzoxazine and polyurethane (100% PU), which resulted in a reduction of 1.31%, 0.99%, and 0.83%, respectively. Based on the results of this study, it can be said that eugenol-based benzoxazine with glycine ethyl ester and urethane significantly improves water absorption property. As a result, this polymer with urethane can act as a better corrosion-protecting coating on the surface of mild steel.

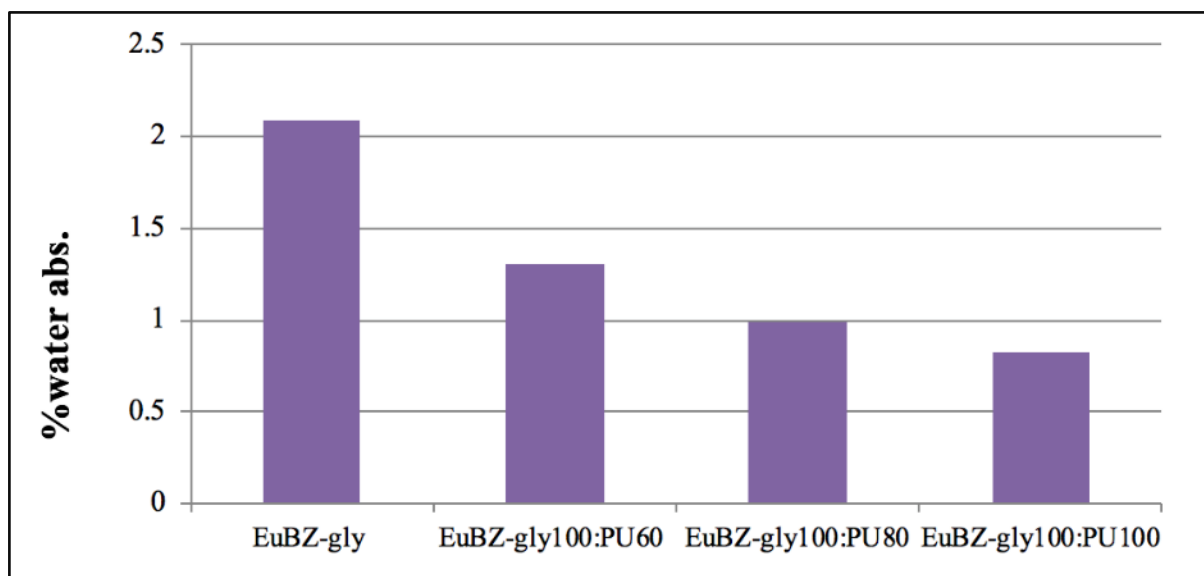


Figure 8: Water absorption experiment results for the Mild steel coated with eugenol based benzoxazine with glycine ethyl ester and its copolymers with 60%, 80% and 100% polyurethane.

3.7 Gel absorption studies

Gel absorption investigations are also important to comprehend the polymer's capacity to create stronger intra-linkages with one another. Because of the decreased porosity, there is less water diffusion into the material. For this work, the monomer and its copolymerized polymers were studied. Figure 9 demonstrates that the monomer alone causes the gel to form with xylene by 81.34%, increasing to 86.67% with the addition of 60% PU, 89.21% with the addition of 80% PU, and 91.13% with the inclusion of an equal quantity of monomer and urethane (100% PU). Based on the outcomes of the enhanced gel absorption, we can conclude that benzoxazine and polyurethane may serve as a superior anticorrosive coating on the mild steel surface.

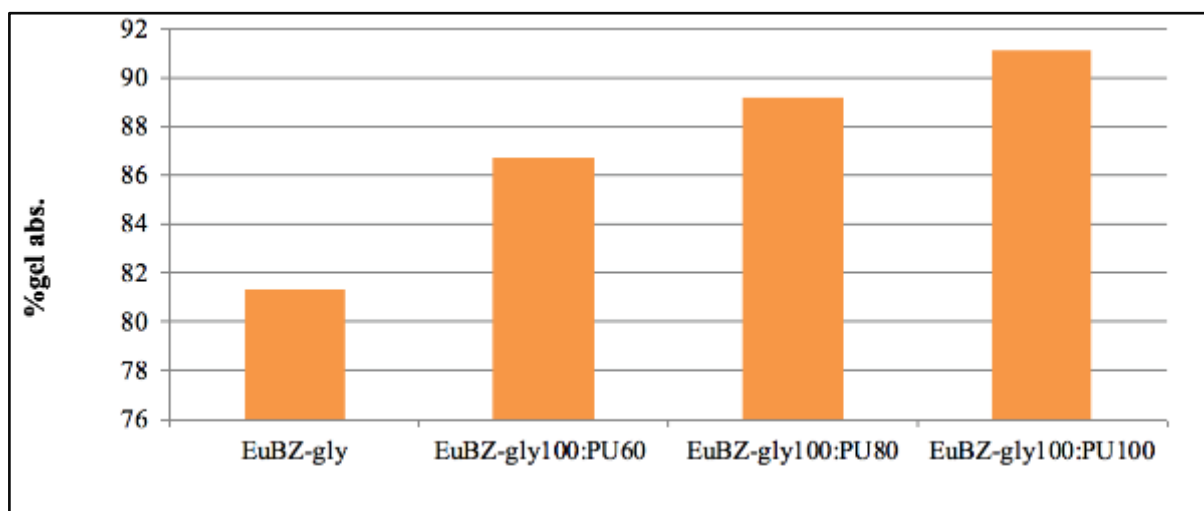


Figure 9: Gel absorption experiment results for the Mild steel coated with eugenol based benzoxazine and its copolymers with 60%, 80% and 100% polyurethane.

3.8 Quantum Chemical Calculations

3.8a- DFT analysis

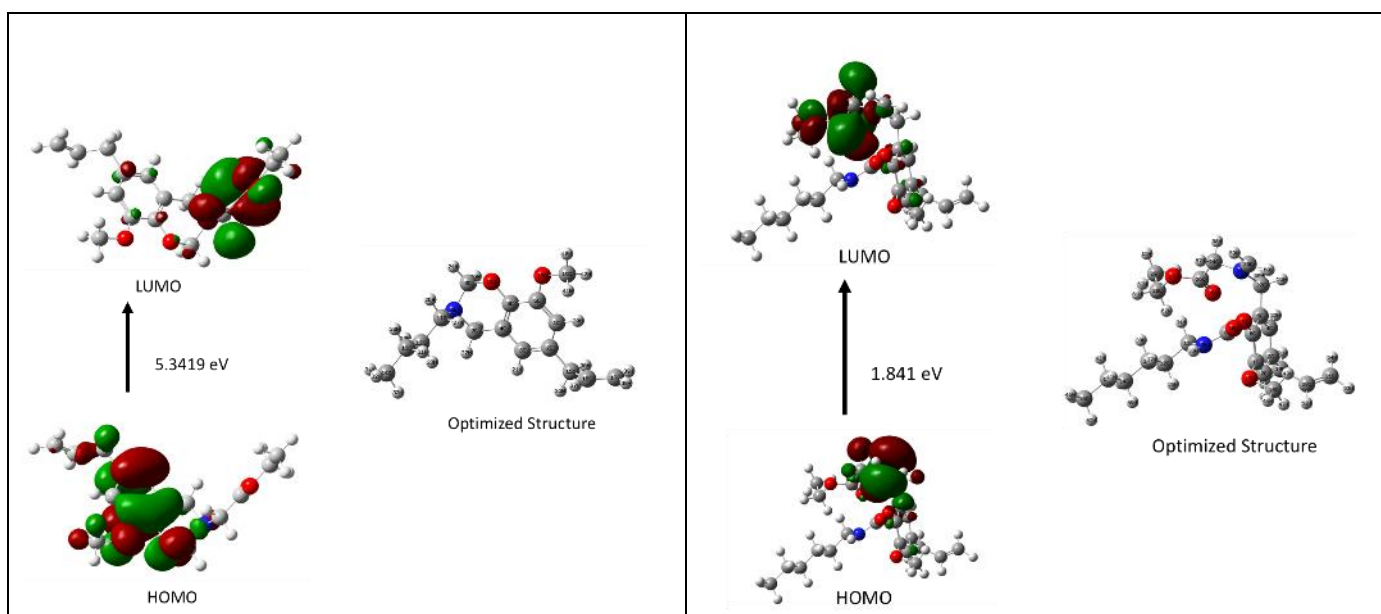
The quantum chemical descriptors of the eugenol-based benzoxazine monomer and its polymerization with hexamethylene isocyanate, including HOMO, LUMO, band gap (ΔE), chemical potential, global hardness (h), global softness (s), electrophilicity index, and dipole moment, are shown in table 3 and figure 10 and figure 11. The ability of a molecule to give electrons is typically connected to the HOMO. If a molecule has a higher HOMO value, it is more likely to transfer electrons to another appropriate molecule that has a low energy or partially filled molecular orbital. Therefore, if a molecule has a higher HOMO value, it will have a greater tendency to donate electrons to the metal's surface, leading to the highest adsorption and the greatest inhibition efficiency. In our experiment shows the E_{HOMO} of EuBZ-gly: PU has greater value than E_{HOMO} of EuBZ, which clearly explains that the polyurethane loaded material shows better inhibition efficiency [40,41].

Table 3: Parameters calculated from DFT studies

Compound name	HOMO	LUMO	Band gap (DE)	Chemical potential	Global hardness	Global softness	Electrophilicity index	Dipole moment (Debye)
Monomer	-5.4976	-0.1556	5.3419	-2.8266	2.6709	0.1871	1.4956	2.4686
Monomer with PU	-2.2610	-0.4198	1.841	-1.3404	0.9205	0.5431	0.9759	5.7566

A molecule with a large band gap (DE) is more stable and associated with low reactivity, while a molecule with a small band gap (DE) is highly reactive, easily polarized, and can thus be readily adsorbed on the surface of a metal. As a result, the efficiency of this type of molecule is high. The value of global hardness (h) and softness (s) can also be used to obtain information about molecular reactivity and selectivity. The HSAB concept serves as the foundation for the relationship between quantum chemical quantities and corrosion inhibition effectiveness. If an inhibitor has a high hardness value or a low softness value, it is regarded as a hard inhibitor. Similar to this, an inhibitor has a low global hardness value and a high

softness value, making it a soft molecule that can readily donate electron density to the acceptor, making it more reactive than a hard inhibitor molecule. Additionally, when an inhibitor has the maximum softness value, adsorption on the metal surface may be simple. In that aspect also, EuBZ-gly: PU (0.5431) > EuBz (0.1871) monomer, which evidently



conclude that the urethane loaded benzoxazine become a good inhibitor than the benzoxazine monomer. According to

definitions, electrophilicity refers to a chemical species' reactivity in attracting electrons from its nucleophile. The opposite of electrophilicity is called nucleophilicity. If an inhibitor molecule having larger electrophilicity value are considered as ineffective towards corrosion inhibition, hence a molecule with small electrophilicity or large nucleophilicity can acts as a good inhibitor. In that aspect also our experiment shows that EuBZ-gly: PU (0.9759) > EuBz (1.4956) monomer, we confirmed the urethane loaded benzoxazine could acts as a better inhibitor than the monomer. Another statistic that is frequently used to forecast the relative effectiveness of corrosion inhibitors is the dipolemoment (m). It measures how polar a bond is and is connected to how many electrons are present in a molecule [41]. Because strong dipole-dipole interactions between inhibitors and the metal result in strong adsorption on the metal's surface, the efficacy of the inhibition is increased. In that aspect also our experiment shows that EuBZ-gly: PU (5.7566) > EuBz (2.4686) monomer, we confirmed the urethane loaded benzoxazine could acts as a better inhibitor than the monomer.

Figure 10: FMO analysis of eugenol based benzoxazine with glycine ethyl ester monomer and its optimized structure

Figure-11: FMO analysis of eugenol based benzoxazine with glycine ethyl ester monomer and its optimized structure along with urethane

3.8b Molecular electrostatic potential (MEP)

By showing the electron distribution on a molecule as a coloured map, the quantum chemical technique may also be used to determine a molecule's chemical reactivity [42]. The colour was used to identify substances having structures that were optimised for positive, negative, and neutral electrostatic potential. Red, yellow, and green can be used to represent a molecule's more negative, somewhat negative, or more positive potential, respectively. Blue symbolises the neutral or zero electron potential of the molecule. From the figures 12 and 13, it is evident that the yellow region around the nitrogen atoms in the molecule and the red colour obtained around the oxygen atoms in the molecule represent the negative potential region that can be adsorbed on the metal surface, respectively.

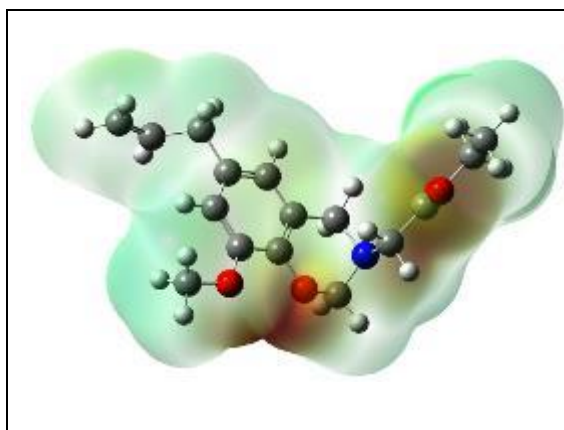


Figure 12: Molecular electrostatic potential mapping of the eugenol based benzoxazine with glycine ethyl ester.

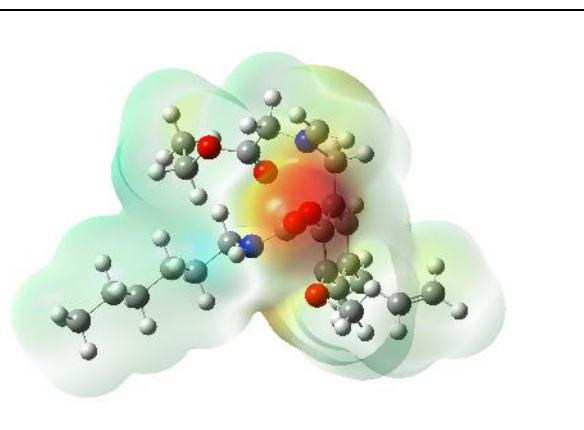


Figure 13: Molecular electrostatic potential mapping of the eugenol based benzoxazine with glycine ethyl ester along with urethane

4. CONCLUSION

We successfully synthesised benzoxazine using glycine ethyl ester, paraformaldehyde, and eugenol, which was then extensively characterised by UV-visible spectroscopy, NMR, and FT-IR. The anti-corrosive characteristics of monomers with copolymers that were 60%, 80%, and 100% urethane loaded were examined, and it was found that the urethane addition enhanced corrosion inhibition on mild steel almost 100% of inhibition efficiency. When the above-synthesised benzoxazine and 100% urethane coating are coupled, the findings for polarisation and impedance show the most effective overall corrosion inhibition. Additional

evidence for the hydrophobic behaviour of the monomer and its copolymers was supplied by studies on water and gel absorption, indicating that polyurethane with a 100% urethane content is hydrophobic and makes a superb anti-corrosive coating on the surface of mild steel. Our efforts to improve the anti-corrosive property of the monomer and its copolymers are supported by the findings of surface morphological studies from SEM, elemental analysis EDAX, and theoretical studies DFT.

ACKNOWLEDGMENTS

The above research has not received any funds or grant from any funding in the public and commercial sectors.

CONFLICT OF INTERESTS


Authors declare that no conflict of interest.

AUTHOR CONTRIBUTIONS

Jayanthi Kannaiyan: Conceptualization, Investigation, Methodology, Writing - Original Draft.

Sivaraju Mani: Supervision, Validation, Review and Editing.

Jayanthi Kannaiyan  <https://orcid.org/0000-0002-1646-1798>

Sivaraju Mani  <https://orcid.org/0000-0001-8502-5458>

REFERENCES:

1. Al-Amiery, Ahmed A., Wan Nor Roslam Wan Isahak, and Waleed Khalid Al-Azzawi. 2023. "Corrosion Inhibitors: Natural and Synthetic Organic Inhibitors" *Lubricants* 11, no. 4: 174. <https://doi.org/10.3390/lubricants11040174>
2. F. EL Hajjaji, E. Ech-chihbi, R. Salim, A. Titi, M. Messali, B. El Ibrahim, S. Kaya, M. Taleb, A detailed electronic-scale DFT modeling/MD simulation, electrochemical and surface morphological explorations of imidazolium-based ionic liquids as sustainable and non-toxic corrosion inhibitors for mild steel in 1 M HCl, *Materials Science and Engineering: B*, Volume 289, 2023, 116232, <https://doi.org/10.1016/j.mseb.2022.116232>.
3. R. Hsissou, O. Dagdag, S. Abbout, et al., Novel derivative epoxy resin TGETET as a corrosion inhibition of E24 carbon steel in 1.0M HCl solution. Experimental and computational (DFT and MD simulations) methods, *Journal of Molecular Liquids*, <https://doi.org/10.1016/j.molliq.2019.03.180>
4. Ramesh Saliyan, V., Adhikari, A.V. Inhibition of corrosion of mild steel in acid media by N'-benzylidene-3-(quinolin-4-ylthio) propanohydrazide. *Bull Mater Sci* 31, 699–711 (2008). <https://doi.org/10.1007/s12034-008-0111-4>.
5. Ambrish Singh, K.R. Ansari, Ismat H. Ali, Brahim EL Ibrahim, Neeta Raj Sharma, Anu Bansal, Abdullah K. Alanazi, Muhammad Younas, Aeshah H. Alamri, Yuanhua

- Lin, Heteroatomic organic compound as a novel corrosion inhibitor for carbon steel in sulfuric acid: Detail experimental, surface, molecular docking and computational studies, *Colloids and Surfaces A: Physicochemical and Engineering Aspects*, Volume 673, 2023, 131692, <https://doi.org/10.1016/j.colsurfa.2023.131692>.
- Al-Moubaraki, A.H.; Chaouiki, A.; Alahmari, J.M.; Al-hammadi, W.A.; Noor, E.A.; Al-Ghamdi, A.A.; Ko, Y.G. Development of Natural Plant Extracts as Sustainable Inhibitors for Efficient Protection of Mild Steel: Experimental and First-Principles Multi-Level Computational Methods. *Materials* **2022**, *15*, 8688. <https://doi.org/10.3390/ma15238688>
 - Shasanowar H Fakir, K Chaitanya Kumar, Hamid Ali, Jaya Rawat, Izharul Haq Farooqi, Synthesis and evaluation of green corrosion inhibitor from rice husk to mitigate corrosion of carbon steel in NaCl environment, *Materials Today: Proceedings*, Volume 82, 2023, Pages 29-37, <https://doi.org/10.1016/j.matpr.2022.11.147>.
 - Mohammad Mobin, Farina Ansar & Mohd Shoeb (2023) Chitosan-polyaniline-TiO₂ ternary nanocomposite coating as effective anti-corrosion material for low carbon steel in 3.5 wt% NaCl solution, *Journal of Adhesion Science and Technology*, DOI: 10.1080/01694243.2023.2179862
 - Vorobyova Victoria, Skiba Margarita and Gnatko Elena, Agri-food wastes extract as sustainable-green inhibitors corrosion of steel in sodium chloride solution: A close look at the mechanism of inhibiting action, *South African Journal of Chemical Engineering* 273 - 295 V - 43, 2023, doi: 10.1016/j.sajce.2022.11.004
 - Ding, Y.; Zhong, J.; Xie, P.; Rong, J.; Zhu, H.; Zheng, W.; Wang, J.; Gao, F.; Shen, L.; He, H.; et al. Protection of Mild Steel by Waterborne Epoxy Coatings Incorporation of Polypyrrole Nanowires/Graphene Nanocomposites. *Polymers* **2019**, *11*, 1998. <https://doi.org/10.3390/polym11121998>
 - Xavier, J.R. High protection performance of vanadium pentoxide-embedded polyfuran/epoxy coatings on mild steel. *Polym. Bull.* **78**, 5713–5739 (2021). <https://doi.org/10.1007/s00289-020-03400-3>
 - Fangjian Gao, Jie Mu, Zhenxiao Bi, Shun Wang, Zili Li, Recent advances of polyaniline composites in anticorrosive coatings: A review, *Progress in Organic Coatings*, Volume 151, 2021, 106071, <https://doi.org/10.1016/j.porgcoat.2020.106071>.
 - Abdelwahed R. Sayed, Mahmoud M. Saleh, Mohammed A. Al-Omair, Hany M. Abd Al-Lateef, Efficient route synthesis of new polythiazoles and their inhibition characteristics of mild-steel corrosion in acidic chloride medium, *Journal of Molecular Structure*, Volume 1184, 2019, Pages 452-461, <https://doi.org/10.1016/j.molstruc.2019.02.061>.
 - Yagci, Y., Kiskan, B. and Ghosh, N.N. (2009), Recent advancement on polybenzoxazine—A newly developed high performance thermoset. *J. Polym. Sci. A Polym. Chem.*, 47: 5565-5576. <https://doi.org/10.1002/pola.23597>
 - C. Zhou, Z. Xin, Chapter 46 - Polybenzoxazine-Based Coatings for Corrosion Protection, *Advanced and Emerging Polybenzoxazine Science and Technology*, Elsevier, 2017, Pages 1003-1017, <https://doi.org/10.1016/B978-0-12-804170-3.00046-9>.
 - Yuzhu Cao, Chen Chen, Xin Lu, Dong Xu, Jian Huang, Zhong Xin, Bio-based polybenzoxazine superhydrophobic coating with active corrosion resistance for carbon steel protection, *Surface and Coatings Technology*, Volume 405, 2021, 126569, <https://doi.org/10.1016/j.surfcoat.2020.126569>.
 - Yang, R., Han, M., Hao, B., Zhang Conceptualization, K., Biobased High-Performance Tri-Furan Functional Bis-Benzoxazine Resin Derived from Renewable Guaiacol, Furfural and Furfurylamine, *European Polymer Journal*, Volume 131, 2020, doi: <https://doi.org/10.1016/j.eurpolymj.2020.109706>.
 - Phalak, G.A., Patil, D.M., Mhaske, S.T., Synthesis and characterization of thermally curable Guaiacol based poly (benzoxazine –urethane) coating for corrosion protection on mild steel,

- European Polymer Journal, Volume 88, 2017, Pages 93-108, <http://dx.doi.org/10.1016/j.eurpolymj.2016.12.030>
19. Madalina-Ioana Necolau , Daniel Grigore , Cristina Stavarache , Jana Ghitman , Elena Iuliana Biru , Horia Iovu, Synthesis And Thermo-Mechanical Characterization Of Vanillin-Based Polybenzoxazines With Complex Architecture, U.P.B. Sci. Bull., Series B, Vol. 85, Iss. 1, 2023. https://www.scientificbulletin.upb.ro/rev_docs_arhiva/fullcc8_548326.pdf
 20. N.K. Sini, Jayashree Bijwe, Indra K. Varma, Thermal behaviour of bis-benzoxazines derived from renewable feed stock 'vanillin', Polymer Degradation and Stability, Volume 109, 2014, Pages 270-277, <https://doi.org/10.1016/j.polymdegradstab.2014.07.015>.
 21. Zhu, H., Hu, W., Zhao, S. et al. Flexible and thermally stable superhydrophobic surface with excellent anti-corrosion behavior. J Mater Sci 55, 2215–2225 (2020). <https://doi.org/10.1007/s10853-019-04050-1>
 22. Sreelakshmi P. Vijayan, Ben John, Sushanta K. Sahoo, Modified cardanol based colorless, transparent, hydrophobic and anti-corrosive polyurethane coating, Progress in Organic Coatings, Volume 162, 2022, 106586, <https://doi.org/10.1016/j.porgcoat.2021.106586>.
 23. X. Lu , Y. Liu , C. L. Zhou , W. F. Zhang and Z. Xin , Corrosion protection of hydrophobic bisphenol A-based polybenzoxazine coatings on mild steel, RSC Adv., 2016, 6 , 5805- 5811, <https://doi.org/10.1039/C5RA22980D>
 24. Arumugam Hariharan, Pichaimani Prabunathan, Ammasai Kumaravel, Manickam Manoj, Muthukaruppan Alagar, Bio-based polybenzoxazine composites for oil-water separation, sound absorption and corrosion resistance applications, Polymer Testing, Volume 86, 2020, 106443, <https://doi.org/10.1016/j.polymertesting.2020.106443>.
 25. Z Wang, S Yao, K Song, X Gong, S Zhang, S Gao, Z Lu, A bio-based benzoxazine surfactant from amino acids, Green Chem., 2020,22, 3481-3488, <https://doi.org/10.1039/D0GC00218F>
 26. Mahendra S. Mahajan, Pramod P. Mahulikar, Vikas V. Gite, Eugenol based renewable polyols for development of 2K anticorrosive polyurethane coatings, Progress in Organic Coatings, Volume 148, 2020, 105826, <https://doi.org/10.1016/j.porgcoat.2020.105826>.
 27. Vikashini Ramesh, Arumugam Hariharan, Krishnasamy Balaji, Govindraj Latha, Manonmani Subbian and Muthukaruppan Alagar (2022) Synthesis, spectral, and thermal studies on eugenol based hydrophobic polybenzoxazines, Polymer-Plastics Technology and Materials, 61:4, 415-425, DOI: 10.1080/25740881.2021.1991951.
 28. P. Thirukumaran, A.Shakila and S. Muthusamy, Synthesis and characterization of novel bio-based benzoxazines from eugenol, RSC Adv., 2014, 4, 7959, DOI: <https://doi.org/10.1039/C3RA46582A>.
 29. M. M. Hussein, S. A. Saafan, N. A. Salahuddin and M. K. Omar, Polybenzoxazine/Mg–Zn nano-ferrite composites: preparation, identification, and magnetic properties, Applied Physics A, 127, 488 (2021), <https://doi.org/10.1007/s00339-021-04620-8>.
 30. Kumar, N., Yadav, N., Amarnath, N. et al. Integrative natural medicine inspired graphene nanovehicle-benzoxazine derivatives as potent therapy for cancer. Mol Cell Biochem 454, 123–138 (2019). <https://doi.org/10.1007/s11010-018-3458-x>.
 31. Chowdaiah, M., Sharma, P. and Dhamodhar, P. A Study on Phytochemicals from Medicinal Plants Against Multidrug Resistant Streptococcus mutans. Int J Pept Res Ther 25, 1581–1593 (2019). <https://doi.org/10.1007/s10989-018-09801-3>
 32. Changlu Zhou, Xin Lu, Zhong Xin, Juan Liu, Yanfeng Zhang, Hydrophobic benzoxazine-cured epoxy coatings for corrosion protection, Progress in Organic Coatings, Volume 76, Issue 9, 2013, Pages 1178-1183, <https://doi.org/10.1016/j.porgcoat.2013.03.013>.
 33. Manoj, M., Kumaravel, A., Mangalam, R. et al. Exploration of high corrosion resistance property of less hazardous pyrazolidine-based benzoxazines in comparison with bisphenol-F

- derivatives. *J Coat Technol Res* 17, 921–935 (2020). <https://doi.org/10.1007/s11998-019-00312-4>
34. Li, S., Zhao, C., Wang, Y. et al. Synthesis and electrochemical properties of electroactive aniline-dimer-based benzoxazines for advanced corrosion-resistant coatings. *J Mater Sci* 53, 7344–7356 (2018). <https://doi.org/10.1007/s10853-018-2113-y>
35. Amani Chrouda, Amel Sbartai, François Bessueille, Louis Renaud, Abderrazak Maaref and Nicole Jaffrezic-Renault, PaperElectrically addressable deposition of diazonium-functionalized antibodies on boron-doped diamond microcells for the detection of ochratoxin A, *Anal. Methods*, 2015,7, 2444-2451 <https://doi.org/10.1039/C4AY02899F>
36. Dinesh Kumar, G., Prabunathan, P., Manoj, M. et al. Fluorine Free Bio-Based Polybenzoxazine Coated Substrates for Oil-Water Separation and Anti-Icing Applications. *J Polym Environ* 28, 2444–2456 (2020). <https://doi.org/10.1007/s10924-020-01782-z>
37. B. Tan, J. He, S. Zhang, C. Xu, S. Chen, H. Liu, W. Li, Insight into anti-corrosion nature of Betel leaves water extracts as the novel and eco-friendly inhibitors, *Journal of Colloid and Interface Science* (2020), doi: <https://doi.org/10.1016/j.jcis.2020.11.059>.
38. R. Sudhakaran, T. Deepa, T. Asokan, M. Govindaraj, T. Kasilingam, S. Babu and A. Sivarajan, Sodium Gluconate As Corrosion Inhibitor For Copper In Potable Water, *Bulletin of Environment, Pharmacology and Life Sciences*, Special Issue [1]2022 : 486-493, [https://bepls.com/special_issue\(1\)2022/74.pdf](https://bepls.com/special_issue(1)2022/74.pdf).
39. Kadhim, A., Al-Okbi, A.K., Jamil, D.M., Qussay, A., Al-Amiery, A.A., Gaaz, T.S., Kadhum, A.A.H., Bakar Mohamad, A., Nassir, M.H., Experimental and theoretical studies of benzoxazines, corrosion inhibitors, *Results in Physics* (2017), doi: <https://doi.org/10.1016/j.rinp.2017.10.027>
40. Savaş Kaya, Burak Tüzün, Cemal Kaya, İme Bassey Obot, Determination of corrosion inhibition effects of amino acids: Quantum chemical and molecular dynamic simulation study, *Journal of the Taiwan Institute of Chemical Engineers*, 58, 2016, 528-535, <https://doi.org/10.1016/j.jtice.2015.06.009>.
41. Y. Sasikumar, A.S. Adekunle, L.O. Olasunkanmi, I. Bahadur, R. Baskar, M.M. Kabanda, I.B. Obot, E.E. Ebenso, Experimental, quantum chemical and Monte Carlo simulation studies on the corrosion inhibition of some alkyl imidazolium ionic liquids containing tetrafluoroborate anion on mild steel in acidic medium, *Journal of Molecular Liquids*, Volume 211, 2015, Pages 105-118, <https://doi.org/10.1016/j.molliq.2015.06.052>.
42. Kadhim, A., Al-Okbi, A.K., Jamil, D.M., Qussay, A., Al-Amiery, A.A., Gaaz, T.S., Kadhum, A.A.H., Bakar Mohamad, A., Nassir, M.H., Experimental and theoretical studies of benzoxazines, corrosion inhibitors, *Results in Physics* (2017), doi: <https://doi.org/10.1016/j.rinp.2017.10.027>